Multi-site coordination N-phosphanylamidine ligands as stabilizers for the synthesis of ruthenium nanoparticles

Raymond Bronger,[a,c] Thanh Dung Le,[b,c] Stéphanie Bastin,[b,c] Jordi García-Antón,[a,c] Cécilia Citadelle,[a,c] Bruno Chaudret,[a,c] Pierre Lecante,[d] Alain Igau*[b,c] and Karine Philippot*[a,c]

Received (in XXX, XXX) 1st January 2007, Accepted 1st January 2007
First published on the web 1st January 2007
DOI: 10.1039/b000000x

The stabilization of ruthenium nanoparticles is achieved by using for the first time multiple donor coordination sites-type ligands, the *N*-phosphanylamidines R"$_2$N–C(R')=N–P(X)R$_2$. These ligands, in which the donor sites are directly connected to one another, lead to the formation of small ruthenium nanoparticles in the size range 1.7-3.1 nm that display narrow size distributions and hexagonal close packed crystalline structure of ruthenium bulk. The characterization of these new samples by a combination of techniques gives information on the surface state of the particles such as the coordination mode of the ligand and the presence of hydrides. CO molecules can also coordinate suggesting that the surface of the particles is not saturated. This work confirms the interest of screening novel ligands for the synthesis of metal nanoparticles and more particularly, of studying their coordination to probe metal nanoparticles' surface properties.

Introduction

The synthesis of well-controlled metal nanoparticles has received an ever-increasing interest in recent years due to their physical and chemical properties that can find applications in various areas.[1] For the past decade, our research has been focused on the organometallic synthesis of well-defined metallic nanoparticles using different types of ligands as stabilizers.[2] Our main objective is to better understand how the ligand can affect the stabilization of the nanoparticles and their surface properties depending on its interaction with the particles surface. To our knowledge, this point has been little studied despite the interest it may present for the development of metal nanoparticles applications such as catalysis.[3] It appears that it is not trivial to test different families of ligands since the study of their interaction at the surface of nanoparticles will help to design ligands able to govern their properties.

In this context, we have been working on metal nanoparticles synthesis in the presence of various ligands having different abilities to interact with nanoparticles surface. Ruthenium is a metal of choice for such a study since it allows us to develop NMR investigations to probe the surface state of the nanoparticles. Until now, ruthenium nanoparticles have been prepared using thiols or amines,[4] diphosphines,[5] diphosphites,[6] 4-(3-phenylpropyl)pyridine[7] and 1,3,5-triaza-7-phosphaadamantane[8] ligands. While thiols, diphosphines and diphosphites ligands gave rise to strong interactions with the metal surface, amines displayed a different behaviour and led to a dynamic ligand exchange. However, a ligand as simple as 4-(3-phenylpropyl)pyridine showed an unexpected mode of stabilization involving π-coordination of the arene groups at the particle surface. This latter stabilization mode specific to compact faces of nanoparticles is not frequent in the literature, and led us to further investigate the use of non classical ligands for nanoparticles synthesis with the aim of providing novel surface properties.

Thus, we chose to use a novel family of functionalized ligands for the synthesis of ruthenium nanoparticles, namely the *N*-phosphanylamidines (phosam) R"$_2$N–C(R')=N–P(X)R$_2$ with X=lone pair, BH$_3$. Theoretical calculations carried out on the *N*-phosphanylamidines (X=lone pair) have shown that the multiple donor sites of these ligands (**L**), which are connected to one another, form a true electronic string. Our experimental studies have demonstrated that the imino nitrogen atom is the basic center of phosams allowing the formation of the corresponding amidinium products **I** (Figure 1).[9] We have reported that *N*-, and *P*-atoms are coordinating sites, **II** and **III** (Figure 1), with *p*-block phosphenium Lewis acid reagents.[10] Even though the phosphino atom is the privilegied donor center to coordinate to *d*-block transition metal **V**,[11] we have evidenced that the imino nitrogen donor site may be involved in the coordination process of the *N*-phosphanyl(form)amidine derivatives **IV** (Figure 1). Moreover, we showed that phosams (R'=Ph) may adopt an η^6-arene-η^1-*P* coordination mode in ruthenium(II) complexes **VI**[12] which evidenced that the phenyl group is also a potential π-coordinating site and that phosams may adapt their coordination mode to the chemical environment around the transition metal.

We may thus expect that all the electron-donor sites of the phosam ligands may interact with the particle surface and therefore lead to a strong stabilizing effect towards these nanoparticles. In order to investigate the influence of the phosam structure on the nanoparticle properties, we prepared phosams with different alkyl chain lengths on the amino nitrogen atom.

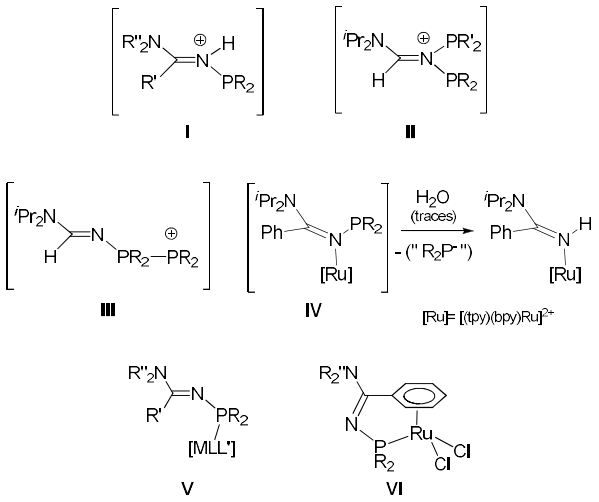

Figure 1. Coordination sites of the *N*-phosphanylamidine derivatives.

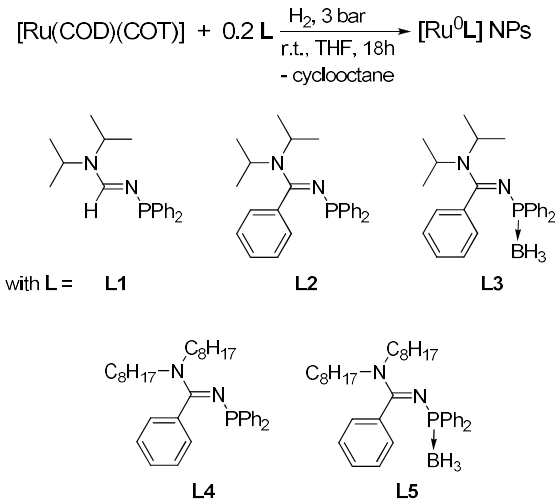

Scheme 1. Synthesis of ruthenium nanoparticles with *N*-phosphanylamidine ligands **L1-L5** as stabilizers.

Results and Discussion

We thus describe here the synthesis of novel ruthenium nanoparticles from the organometallic precursor [Ru(COD)(COT)] (COD = 1,5-cyclooctadiene; COT = 1,3,5-cyclooctatriene) stabilized by *N*-phosphanylamidines (phosams). The decomposition of [Ru(COD)(COT)] was performed at room temperature under dihydrogen atmosphere according to our previously reported methodology.[4,5] The ambidentate ligands **L1-L5** were added to the reaction medium in a molar ratio [L]/[Ru]=0.2 (Scheme 1) giving rise to nanoparticle samples **Ru1-Ru5**. The initial pale-yellow solutions became black in a few minutes after hydrogen introduction, confirming decomposition of the ruthenium complex. Optimized conditions led to reproducible nanoparticles syntheses in quantitative yields. These ruthenium nanoparticles could be isolated as black powders after pentane precipitation and washings. They were characterized by Transmission Electron Microscopy (TEM), Wide-Angle X-ray Scattering (WAXS), elemental analysis, Infra-Red (IR) and for some of them Nuclear Magnetic Resonance (NMR). The characteristics of the particles are summarized in Table 1.

TEM images of the so-obtained nanoparticles and the corresponding size histograms are presented in Figure 2 and in Figures S1, S2 and S3 in the Supporting Information. These nanoparticles are well-dispersed on the grids and present mean sizes comprised between 1.7(0.2) and 3.1(0.3) nm depending on the ligand. While the observed nanoparticles are spherical for **Ru2** and **Ru3** samples, they display a slightly more elongated shape for samples **Ru1**, **Ru4** and **Ru5**. This seems to indicate that the ligands have a different stabilizing behaviour.

The WAXS analyses revealed well-crystallized ruthenium nanoparticles displaying hexagonal compact (hcp) structure as for ruthenium bulk. The observed coherence lengths are in good to very good accordance with the mean sizes determined by TEM measurements, as shown for example for sample **Ru1** in Figure 3. In this case, the mean diameter resulting from TEM and the coherence length from WAXS have the same 2.5 nm value. This indicates a crystalline character of the whole particle.

Table 1. Characteristics of Ru NPs stabilized with ligands **L1-L5**.

Sample	Mean diameter (nm) determined by TEM	Coherence length (nm) determined by WAXS	Elemental analysis Ru and P (%wt)	IR (cm^{-1})[a] after exposure under CO	Surface Hydrogen Atoms (%)	H atom/ surface Ru atom	^{31}P MAS NMR (ppm)
Ru1	2.4 (0.2)	2.5	56.87; 2.48	1994	38	0.9	50
Ru2	3.1 (0.3)	2.5	46.31; 3.65	1999	52	1.5	-20
Ru3	2.2 (0.3)	1.6	46.57; 3.85	2001	60	1.3	-20 (major) 60; 20 (minor)
Ru4	2.0 (0.2)	<2	48.17; 3.69	nd	nd	nd	nd
Ru5	1.7 (0.2)	1.9	nd	nd	nd	nd	nd

[a] CO band observed after exposure under CO (3 bar; 48h). nd = not determined

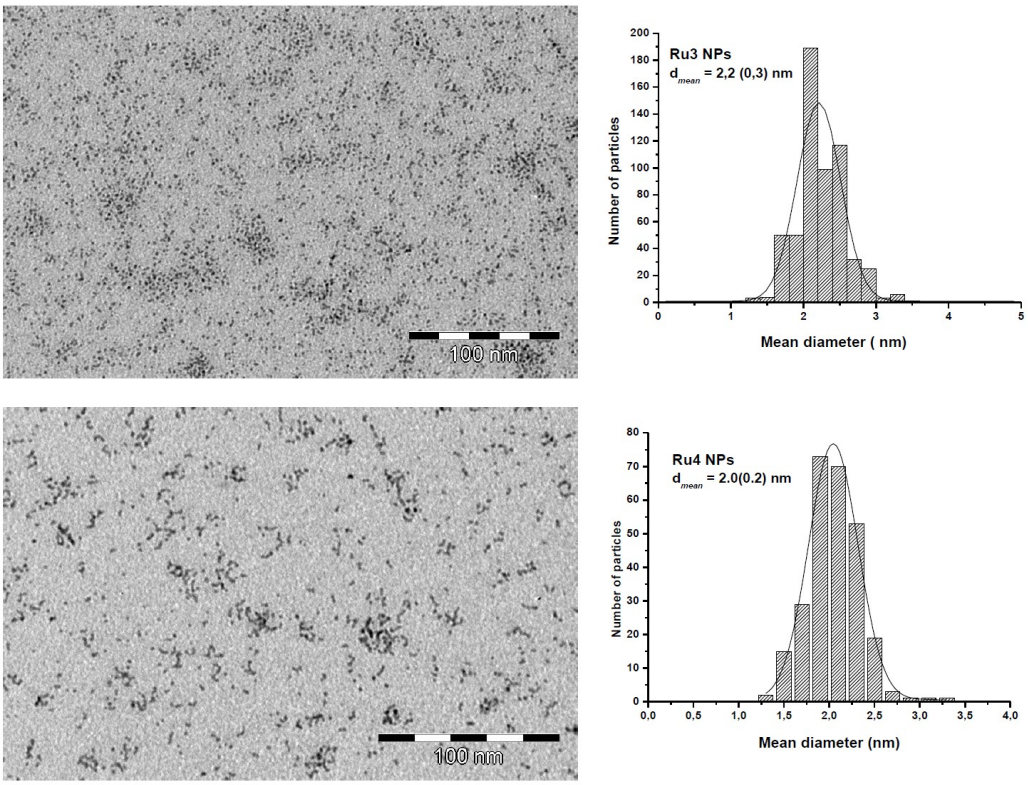

Figure 2. TEM images of *N*-phosphanylamidine-stabilized ruthenium nanoparticles **Ru3** and **Ru4** and corresponding size histograms.

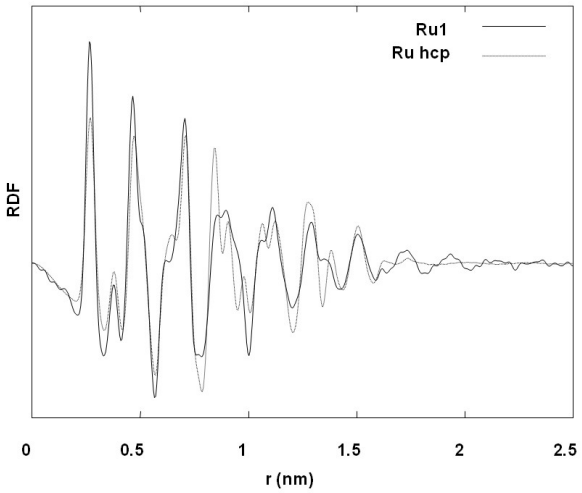

Figure 3. WAXS analysis of *N*-phosphanylamidine-stabilized ruthenium nanoparticles **Ru1** in comparison with theoretical hcp ruthenium

Elemental analyses were performed on the purified nanoparticles **Ru1**-**Ru4** to determine the ruthenium and the phosphorus contents (Table 1). The presence of phosphorus confirms that the ligands are present on the particles surface after the purification step and indicates that they are thus strongly attached. Thanks to the elemental analyses data we could determine the [P]/[Ru] ratio and further the approximate number of ligands coordinated at the particle surface. These numbers were estimated taking into account the mean diameters of the particles deduced from TEM observations and are only indicative (see experimental part). These numbers are different depending on the ligand used as stabilizer. Calculation of the [L]/[$Ru_{surface}$] ratios gives rise to a value of 0.32 for **Ru1**, 0.71 for **Ru2**, 0.59 for **Ru3** and 0.47 for **Ru4**. A comparison of the numbers obtained for **Ru2** (0.71) and **Ru4** (0.47) may indicate a lower number of ligands at the particles surface when long alkyl chains are present in the ligand which is expected as such ligands are more bulky. Another hypothesis could be a coordination of the ligand in a second coordination sphere in the case of **Ru2**.

The presence of the ligands at the particles surface was also attested by IR studies (KBr pellets) recorded on the powders obtained after purification of the nanoparticles. In the case of **Ru3**, the characteristic υ_{BH} (asym and sym) absorption bands of the BH_3 group expected in the 2370-2280 cm^{-1} region are absent, which suggests that the BH_3 group has been eliminated during the particles synthesis (Figure 4).

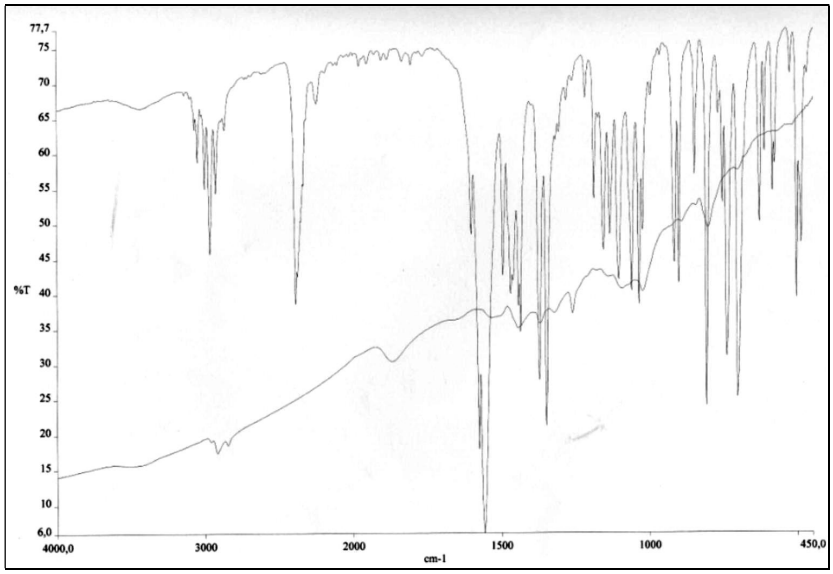

Figure 4. IR spectra recorded for **L3** ligand (top) and **Ru3** nanoparticles (bottom).

The exposure of the nanoparticles to a CO atmosphere (3 bar, 48h) gave rise to the presence of a CO stretch in the IR spectra in the range of 1994-2001 cm^{-1}. This band may be attributed to the coordination of CO at the surface of Ru nanoparticles in a bridging mode as previously observed with other systems.[4] This indicates that the surface of the nanoparticles is not saturated.

As the nanoparticles are prepared from decomposition of [Ru(COD)(COT)] under dihydrogen, the presence of hydrogen atoms adsorbed at the surface of the ruthenium nanoparticles was expected. To quantify these hydrogen atoms, fresh colloidal solutions of samples **Ru1**-**Ru3**, previously degassed by performing five vacuum/argon bubbling cycles, were used to hydrogenate 2-norbornene without further addition of dihydrogen gas to the reaction media. Thus, in these conditions, only the hydrogen atoms present at the surface of the particles may act as reducing agents. The conversion into norbornane was determined by gas chromatography after 24h of reaction. From 2-norbornene conversion, taking into account the quantity of introduced ruthenium, we could evaluate the percentage of hydrogen atoms present at the surface of the particles. These experiments led to 38, 52 and 60% of hydrogen atoms compared to ruthenium ones in the particles for **Ru1**, **Ru2** and **Ru3** respectively. In other terms these percentages correspond to 0.9, 1.5 and 1.3 H per surface ruthenium atom for **Ru1**, **Ru2** and **Ru3** respectively. These values are close to the ones obtained for ruthenium nanoparticles stabilized with hexadecylamine or diphosphinodecane for which numbers of 1.3 and 1.1 were found respectively.[5]

Solid state ^{31}P NMR studies have been carried out on **Ru1**, **Ru2** and **Ru3** samples (Figure 5). The spectrum recorded for **Ru1** revealed a broad signal centered at 50 ppm. This chemical shift strongly suggests the P-coordination of **L1** on the surface of the NPs. Indeed, the coordination chemistry of **L1** on transition metal led to the formation of the resulting *P*-coordinated *N*-phosphanylformamidine complexes with a chemical shift in the range of 50 ppm.[13] In marked contrast, for **Ru2** a broad peak centered at –20 ppm is observed by ^{31}P NMR. This chemical shift is in the range of the signals detected for diaryl phosphanide moiety Ar_2P associated with metals.[14] The phosphanide fragment PPh_2 may result from the cleavage of the N–P linkage in *N*-phosphanylamidine ligand **L2** which then coordinates on the surface of the NPs. It is noteworthy that the amidine organic moiety $^{i}Pr_2N$–C(Ph)=N– which is released in the cleavage process may also act as a potential ligand and coordinate as well onto the surface of the NPs via the imino nitrogen atom, but this was not detected. In the case of **Ru3**, the ^{31}P NMR spectrum showed one major signal centered at -20 ppm. This chemical shift, identical to the one observed in the experiment above involving ligand **L2**, could be explained by the decomplexation of the borane fragment BH_3 from the phosphorus atom in ligand **L3** to form in situ the corresponding ligand **L2**. However it is important to note that the structural characteristics of the nanoparticles obtained from **L2** and **L3** are different. It is well known that amino-borane and phosphino-borane complexes act as reducing agents in the presence of metals as for example the reduction of Pd(II) compound to Pd(0).[15] The presence of borane organic derivatives during the process of the formation of the nanoparticles **Ru3** may explain the difference in size of the nanoparticles obtained for **Ru2**. The two other minor signals observed for **Ru3** at 60 and 20 ppm may correspond respectively to a small fraction of the *P*-coordinated **L2** generated in situ and to its oxidation product, the $^{i}Pr_2N$–C(Ph)=N–P(O)Ph_2 phosphine oxide, which coordinated onto the NPs surface.[16]

From ^{31}P MAS NMR and hydrogen quantification results, we can anticipate in a first approach that the π-coordination of the phenyl ring in ligands **L2** and **L3** is not involved in the formation of nanoparticles **Ru2** and **Ru3** as the measured percentages of hydrogen atoms on the surface of the NPs are higher for these nanoparticles compared to **Ru1**. Indeed, we may have expected in

the case of π-coordination a more pronounced coverage of ligands **L2** and **L3** which would have induced a lower quantity of hydrogen adsorbed at the surface of the NPs compared to ligand **L1**. This observation is in favour of the cleavage of ligand **L2** into two fragments with *P*-coordination of the phosphanide fragment Ph_2P and, possibly the *N*-coordination of the amidine moiety.

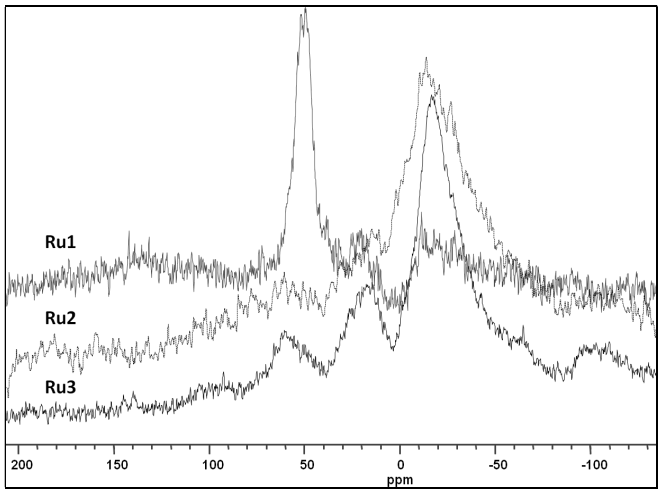

Figure 5. ^{31}P NMR spectra of *N*-phosphanylamidine-stabilized ruthenium nanoparticles.

In summary, *N*-phosphanylamidines ligands are able to act as stabilizers for the synthesis of ruthenium nanoparticles giving rise to small nanoparticles in the range 1.7-3.1 nm. Like previously described for ruthenium nanosystems, these novel nanoparticles present hydrides at their surface and can coordinate CO. The NMR analyses carried out with some of the obtained samples indicate that the fate of the ligand on the particle surface may be different depending on its nature. An evolution of the stabilizing ligand has already been observed in the case of diphosphine-stabilized RuNPs, for which a partial hydrogenation of the phenyl rings of the ligands was observed by NMR. Such a hydrogenation of the aromatic part of the ligands could be explained by their proximity to the particles surface where hydrides are coordinated or by a catalyst behavior of neigbouring NPs. In the present case, the fate of the ligand is more drastic. NMR data are in favor of the coordination of the ligands at the particles surface through their phosphorus atoms. For **Ru1**, the ^{31}P chemical shift clearly indicates a classical coordination of the N-phosphanylamidine ligand **L1** by the phosphorus atom. In the case of **Ru2** and **Ru3,** the NMR data show that the ligands **L2** and **L3** have reacted upon coordination on the surface of the particles resulting into a drastic change of their original structure. For **Ru2**, ^{31}P NMR data are in favor of the coordination of a phosphanide ($–PPh_2$) fragment that would result from cleavage of the N–P bond of the initial ligand. Such cleavage may take place at the surface of the particles. For **Ru3**, IR data are in agreement with the decomplexation of the borane fragment $-BH_3$ from the phosphorus atom in ligand **L3** that would lead to the corresponding **L2** ligand. In addition, ^{31}P NMR data obtained for **Ru3** are also in favor of the coordination of a phosphanide $–PPh_2$ fragment resulting from cleavage of the N–P bond of the ligand. Such a difference in the fate of the ligand comparing **Ru1** with **Ru2**/**Ru3** in which the ligand structure differs only by a phenyl ring in β position to phosphorus atom, may be explained by the transient formation of a chelating η^6-phenyl-η^1-P intermediate [12] at the particle surface giving rise to an important structural tension of the amidine skeleton that induced the cleavage of the N-P bond of the ligand.

Conclusions

In this paper, we describe the organometallic synthesis of ruthenium nanoparticles using as stabilizing agent a novel class of ligands which incorporate in their structure multiple coordination sites directly connected to one another, namely the *N*-phosphanylamidines $R''_2N–C(R')=N–P(X)R_2$. Our results show that these amidine ligands are able to act as stabilizers since small ruthenium nanoparticles in the size range 1.7-3.1 nm that display narrow size distributions are obtained. The characterization of the so-obtained samples gives information on the surface state of the particles and on the coordination of the ligands at their surface. As observed for previously described ruthenium nanoparticles, hydrides are present at the particle surface in a quantity similar as for known systems. IR data after exposure of the nanoparticles under CO atmosphere reveal that CO molecules are able to coordinate at their surface suggesting that the surface of the particles is not saturated. MAS NMR investigations show that the coordination of the ligands takes place probably through their phosphorus atoms. But, depending on the ligand, a different fate of the stabilizer is observed giving rise in some cases to a drastic cleavage of the N–P linkage. This work confirms the interest of studying novel families of ligands to tune metal nanoparticles' surface properties.

Experimental Section

General information and methods: All manipulations were carried out under inert atmosphere with standard vacuum and dry-argon techniques in Schlenk or Fischer-Porter glassware or in a glove-box. The reactive agents were purchased as following: ruthenium chloride monohydrate from Strem Chemicals; 1,5-cyclooctadiene from Acros Organics; zinc from Merck; silanized silica gel from Merck and chlorodiphenylphosphane (97%) from Alfa Aesar and distilled prior to use. All other commercial chemicals were purchased from Aldrich and were used as received. All solvents were analytical grade and used freshly distilled: THF over sodium-benzophenone; pentane and CH_2Cl_2 over calcium hydride; $CDCl_3$ over P_2O_5; C_6D_6, CD_2Cl_2 (Euriso-top) and other solvents stored on 4 Å molecular sieves. All reagents and solvents were degassed before use by means of three freeze-pump-thaw cycles. The ruthenium 1,5-cyclooctadiene 1,3,5-cyclooctatriene complex, [Ru(COD)(COT)], was synthesized as previously described.[17] The synthesis of ligands **L1**[9] and **L2**[12] was performed as previously reported, while the synthesis of ligands **L3**-**L5** is hereafter described.

Concerning the ligands, liquid NMR spectra were recorded on a Bruker AV 300 or AC200 spectrometers. Chemicals shifts for ^1H and ^{13}C are referenced to residual solvent resonances used as an internal standard and reported relative to $SiMe_4$. ^{31}P chemical shifts are reported relative to external aqueous 85% H_3PO_4 (^{31}P). All the ^1H and ^{13}C signals were assigned on the basis of chemical shifts, spin-spin coupling constants, splitting patterns and signal

intensities, and by using 2D experiments such as $^1H–^1H$ COSY45, $^1H–^{13}C$ HMQC and $^1H–^{13}C$ HMBC experiments. All spectra were recorded at ambient probe temperature unless stated otherwise. Crude reaction mixtures were controlled by NMR in CH_2Cl_2 with a sealed tube of toluene-d_8 as a reference. All compounds were then fully characterized in the deuterated solvent stated in the experimental part. For ruthenium nanoparticles, solid-state NMR spectra were recorded on a Bruker Advance 400.

Mass chromatograms were obtained on a HP 6890 Series GC system with a HP5MS Agilent nonpolar 95% dimethyl polysiloxane capillary column of 30m×0.25mm×0.25µm and a 70 eV electronic impact detector. Mass spectra of ligands were recorded on a TSQ7000 Thermo Electron (EI and DCI).

Gas chromatograms were obtained on a HP 5890 Series II Gas Chromatograph with a SGE BP1 non polar 100% dimethyl polysiloxane capillary column of 50m×0.32mm×0.25µm. The method used for 1-octene/octane experiments consists in an initial isothermal period at 70° C for 10 mins followed by a 8°C/min temperature ramp to 250 °C. The method used for 2-norbornene/norbornane experiments consists in an initial isothermal period at 40° C for 15 mins followed by a 8°C/min temperature ramp to 250 °C.

Melting points were obtained using an Electrothermal Digital Melting Point apparatus and are uncorrected.

Infrared spectra were recorded on a Perkin-Elmer IRFT GX 2000 spectrophotometer as solutions transferred into a KBr cell or using KBr pellets after isolation of the products as solids. The reference spectrum of the solvent was systematically subtracted.

Transmission Electron Microscopy at low (TEM) and high resolution (HRTEM) analyses were performed at the "Service Commun de Microscopie Electronique de l'Université Paul Sabatier" (TEMSCAN). TEM images were obtained using a JEOL 200CX-T electron microscope operating at 200 kV with resolution point of 4.5. HRTEM observations were carried out with a JEOL JEM 2010 electron microscope working at 200 kV with a resolution point of 2.5 Å. Samples for TEM/HREM analyses were prepared by slow evaporation of a drop of crude colloidal solution deposited under argon onto holey carbon-covered copper grids. The size distributions were determined through a manual analysis of enlarged micrographs by measuring ca. 300 particles on a given grid to obtain a statistical size distribution and a mean diameter.

Data collection for the Wide-Angle X-Ray Scattering (WAXS) was performed on small amounts of powder at the CEMES-CNRS (Toulouse). The samples were sealed in 1 mm diameter Lindemann glass capillaries. The measurements of the X-ray intensity scattered by the samples irradiated with graphite-monochromatized molybdenum Kα (0.071069 nm) radiation were performed using a dedicated two-axis diffractometer. Radial distribution functions (RDF) were obtained after Fourier Transformation of the reduced intensity functions. The crystalline structure was determined through comparison with theoretical hcp Ru (JCPDS-6-663).

Elemental analyses were performed at the "Service Central d'Analyses" of CNRS (Vernaison, France) to obtain Ruthenium and Phosphorus contents, and at the "Service d'Analyses" at the "Laboratoire de Chimie de Coordination" in Toulouse to get hydrogen and carbon ones.

Synthesis of ligand L3: To a diethyl ether solution (10 mL) of *N*-phosphanylamidine **2** (4.623 g, 11.90 mmol) at 0°C was added a 1.0 mol.L^{-1} solution of BH_3•THF (11.9 mL, 11.90 mmol). The reaction mixture was stirred for 30 min and the volatiles were removed under vacuum. The residue was washed with pentane (3 × 10 mL) and then purified by column chromatography on silica gel (eluent Et_2O/pentane: 80/20). The *N*-phosphanylamidine borane adduct **L3** was isolated in 78% yield as a pale yellow powder. M.p. 188 °C. IR (KBr): ν = 1558 cm–1 (C=N). $^{31}P\{^1H\}$ NMR (101.2 MHz, $CDCl_3$, 25°C): δ = 46.1 (br d, $^1J_{PB}$ = 88.5 Hz) ppm. ^1H NMR (200.1 MHz, $CDCl_3$, 25°C): δ = 1.04 (d, $^3J_{HH}$ = 6.8 Hz, 6 H, NCHC*H*$_3$), 1.74 (d, $^3J_{HH}$ = 6.8 Hz, 6 H, NCHC*H*3), 3.57 (sept, $^3J_{HH}$ = 6.8 Hz, 1 H, NC*H*CH3), 3.74 (sept, $^3J_{HH}$ = 6.8 Hz, 1 H, NC*H*CH3), 6.75–7.62 (m, 15 H, H_{Ph}) ppm. $^{13}C\{^1H\}$ NMR (50.3 MHz, $CDCl_3$, 25°C): δ = 20.4 (s, NCH*C*H3), 46.8 (s, N*C*HCH3), 51.5 (s, N*C*HCH3), 126.5 (s, C_{Ph}), 127.8 (d, J_{CP} = 10.6 Hz, C_{Ph}), 128.2 (s, C_{Ph}), 129.6 (s, C_{Ph}), 131.7 (d, J_{CP} = 10.5 Hz, C_{Ph}), 135.6 (d, J_{CP} = 7.3 Hz, C_{Ph}), 136.9 (d, J_{CP} = 64.8 Hz, *i*-PC_{Ph}), 166.3 (d, $^2J_{CP}$ = 6.9 Hz, Ph*C*=N) ppm. $C_{25}H_{32}BN_2P$ (402.32): calcd. C 74.63, H 8.02, N 6.96; found C 75.02, H 8.15, N 6.78. EI MS: m/z = 388 $[M – BH_3]^+$.

Synthesis of ligand L4: To a toluene solution (10 mL) of **L5** (0.586 g, 1.080 mmol) was added at room temperature, 0.121 g (1.080 mmol) of 1,4-diazabicyclo-[2.2.2]-octane (Dabco). The reaction mixture was stirred and heated under reflux for 3.5 h. The volatiles were removed under vacuum and **L4** was isolated after extraction with pentane (3 × 5 mL) as a white oil in 97% yield. $^{31}P\{^1H\}$ NMR (101.2 MHz, $CDCl_3$, 25 °C): δ = 35.0 (s) ppm. ^1H NMR (300.1 MHz, $CDCl_3$, 25°C): δ = 0.96–1.90 (m, 30 H, $N(CH_2(CH_2)_6CH_3)_2$), 3.11 (m, 2 H, $N(CH_2(CH_2)_6CH_3)_2$), 3.84 (m, 2 H, $N(CH_2(CH_2)_6CH_3)_2$), 7.01–7.63 (m, 15 H, H_{Ph}). $^{13}C\{^1H\}$ NMR (75.5 MHz, $CDCl_3$, 25°C): δ = 14.2 (s, C_{octyl}), 22.7 (s, C_{octyl}), 26.9–29.8 (m, C_{octyl}), 31.9 (s, C_{octyl}), 47.4 (br s, C_{octyl}), 49.9 (br s, C_{octyl}), 127.0 (d, J_{CP} = 3.2 Hz, C_{Ph}), 127.7 (s, C_{Ph}), 127.8 (d, J_{CP} = 6.7 Hz, C_{Ph}), 128.2 (s, C_{Ph}), 128.3 (s, C_{Ph}), 131.0 (d, J_{CP} = 20.9 Hz, C_{Ph}), 137.1 (d, J_{CP} = 8.8 Hz, C_{Ph}), 145.6 (d, J_{CP} = 13.1 Hz, C_{Ph}), 166.8 (d, $^2J_{CP}$ = 29.5 Hz, Ph*C*=N) ppm. DCI(CH_4) MS: m/z = 529 $[M+H]^+$.

Synthesis of ligand L5: A solution of *n*-BuLi (3.81 mL, 6.100 mmol) was added slowly at –40 °C to a solution of *n*-Oc_2NH (1.84 mL, 6.100 mmol) in 20 mL of diethyl ether. After 10 min at room temperature, the reaction mixture was cooled down to 0°C and a solution of benzonitrile (0.628 g, 6.100 mmol) in 5 mL of diethyl ether was added dropwise. The yellow solution was stirred for 3 h at 0 °C. The chlorophosphane Ph_2PCl (1.346 g, 6.100 mmol) was then added dropwise. The reaction mixture was allowed to warm to room temperature and a white precipitate of LiCl was formed. To this reaction mixture cooled at 0 °C, a 1.0 mol.L^{-1} solution of BH_3•THF (6.10 mL, 6.100 mmol) was added. The volatiles were removed under vacuum. The residue was purified by column chromatography on silica gel (eluent Et_2O/pentane 4/96). The *N*-phosphanylamidine borane adduct **L5** was isolated in 56% yield as a white oily liquid. $^{31}P\{^1H\}$ NMR (81.0 MHz, $CDCl_3$, 25°C): δ = 47.4 (br s) ppm. ^1H NMR (200.1 MHz, $CDCl_3$, 25°C): δ = 0.76–1.47 (m, 28 H,

N(CH_2(CH_2)$_6$$CH_3$)$_2$), 1.90 (m, 2 H, N($CH_2$($CH_2$)$_6$$CH_3$)$_2$), 2.99 (t, $^3J_{HH}$ = 7.6 Hz, 2 H, N(CH_2(CH_2)$_6$$CH_3$)$_2$), 3.80 (t, $^3J_{HH}$ = 7.6 H, 2 H, N(CH_2(CH_2)$_6$$CH_3$)$_2$), 6.82–7.97 (m, 15 H, H_{Ph}). NMR $^{13}C\{^1H\}$ (50.3 MHz, $CDCl_3$, 25°C): δ = 14.0 (s, C_{octyl}), 14.1 (s, C_{octyl}), 22.6 (s, C_{octyl}), 22.7 (s, C_{octyl}), 26.5 (s, C_{octyl}), 27.2 (s, C_{octyl}), 27.4 (s , C_{octyl}), 28.9 (m, C_{octyl}), 29.0 (s, C_{octyl}), 29.4 (s, C_{octyl}), 29.5 (s, C_{octyl}), 31.6 (s, C_{octyl}), 31.9 (s, C_{octyl}), 47.4 (s, C_{octyl}), 50.0 (s, C_{octyl}), 127.1 (s, C_{Ph}), 127.7 (s, C_{Ph}), 127.9 (s, C_{Ph}), 128.5 (s, C_{Ph}), 129.7 (s, C_{Ph}), 129.7 (s, C_{Ph}), 131.5 (d, J_{CP} = 10.2 Hz, C_{Ph}), 134.6 (d, J_{CP} = 6.1 Hz, C_{Ph}), 136.8 (d, $^1J_{CP}$ = 65.5 Hz, C_{Ph}), 166.8 (d, $^2J_{CP}$ = 8.7 Hz, Ph*C*=N) ppm. $C_{35}H_{52}BN_2P$ (542.59): calcd. C 77.48, H 9.66, N 5.16; found C 77.98, H 9.72, N 5.45. DCI(NH_3) MS: m/z = 543 $[M+H]^+$.

Typical procedure for the synthesis of ruthenium nanoparticles: As a standard procedure, [Ru(cod)(cot)] (150mg, 0.476 mmol) was dissolved under an atmosphere of argon at –110ºC (ethanol/N_2 bath) in tetrahydrofuran (150 mL) containing the chosen ligand (molar ratio [L]/[Ru]=0.2) in a closed pressure bottle. The Fischer-Porter reactor was then pressurized at r.t. under dihydrogen (3 bar) for 30 min. The initial yellow solution became black after 1h. Vigorous magnetic stirring was maintained for 18 h. After that period of time, the hydrogen pressure was eliminated, and a drop of the crude colloidal solution was deposited under an argon atmosphere on a holey carbon-covered copper grid for electron microscopy analysis. Precipitation with a tetrahydrofuran/pentane mixture at low temperature gave rise to black precipitates that were washed with cold pentane (3 × 5mL) and dried under vacuum.

Ru1: The synthesis of **Ru1** was completed according to the general procedure using ligand L1 (36.5 mg, 0.0952 mmol) as stabilizing agent. The product was isolated as a black powder (41 mg). TEM: mean diameter = 2.4 (0.2) nm; Elemental analysis: %Ru = 56.87, %P = 2.48 and calculated formula [Ru_{561}(THF)$_x$(**L1**)$_{80}$] and [**L1**]/[Ru_s]=80/252=0.32. IR: 1994 cm^{-1} (νC=O) after sample exposure under CO pressure (3 bar) for 2 days.

Ru2: The synthesis of **Ru2** was completed according to the general procedure using ligand **L2** (37 mg, 0.0952 mmol) as stabilizing agent. The product was isolated as a black powder (39 mg). Mean diameter = 3.1(0.3) nm. Elemental analysis: %Ru = 46.31, %P = 3.65 and calculated formula [Ru_{1415}(THF)$_x$(**L2**)$_{353}$] and [**L2**]/[Ru_s]=353/642=0.71. IR: 1999 cm^{-1}. (νC=O) after sample exposure under CO pressure (3 bar) for 2 days.

Ru3: The synthesis of **Ru3** was completed according to the general procedure using ligand **L3** (37 mg, 0.0952 mmol) as stabilizing agent. The product was isolated as a black powder (34 mg). TEM: Mean diameter = 2.2 (0.3) nm; Elemental analysis: %Ru = 46.57, %P = 3.85 and calculated formula [Ru_{561}(THF)$_x$(**L3**)$_{151}$] and [**L3**]/[Ru_s]=151/561=0.59. IR: 2001 cm^{-1}. (νC=O) after sample exposure under CO pressure (3 bar) for 2 days.

Ru4: The synthesis of **Ru4** was completed according to the general procedure using ligand **L4** (50 mg, 0.0952 mmol) as stabilizing agent. The product was isolated as a black powder (38 mg). TEM: Mean diameter = 2.0(0.2) nm. Elemental analysis: %Ru = 48.17, %P = 3.69 and calculated formula [Ru_{309}(THF)$_x$(**L4**)$_{77}$] and [L4]/[Ru_s]=77/162=0.47.

Ru5: The synthesis of **Ru5** was completed according to the general procedure using ligand **L5** (52 mg, 0.0952 mmol) as stabilizing agent. The product was isolated as a black powder (37 mg). TEM: Mean diameter = 1.7(0.2) nm.

Quantification of Hydrides at the surface of ruthenium nanoparticles: The general procedure for the preparation of reaction mixtures for the quantification of hydrogen atoms adsorbed onto the surface of Ru nanoparticles by GC analyses was the following. Each colloidal solution has been prepared in THF as previously described. On each fresh colloidal solution, five cycles of 1 minute vacuum/1 minute bubbling of argon were performed in order to eliminate the dihydrogen solved into the solvent. Then, 5 molar equivalents of olefin (2-norbornene), previously filtered through alumina, were added and the reaction medium was stirred at room temperature. Samples were regularly taken from the solutions after 24 hours for GC analyses and estimation of the olefins conversion into alkanes. To get nanoparticle-free solutions, filtration of the samples was realized through an Al_2O_3 pad. The quantification of hydrides has been performed with ruthenium nanoparticle systems **Ru1**, **Ru2** and **Ru3**, taking into account the quantity of introduced ruthenium.

Acknowledgments

The authors thank V. Collière and L. Datas (UPS-TEMSCAN) for TEM/HRTEM, Y. Coppel and S. Parres-Maynadié (LCC-CNRS) for solution and solid-state NMR, J.F. Meunier (LCC-CNRS) for TGA analyses and the CNRS for financial support. R. Bronger thanks EC for Marie-Curie individual fellowship (MEIF-CT-2006; n°23753). T. D. L. acknowledges the Agence Universitaire de la Francophonie (AUF) for a PhD fellowship.

Notes and references

[a] Nanostructures and Organometallic Chemistry Group, CNRS; LCC (Laboratoire de Chimie de Coordination); 205 Route de Narbonne, F-31077 Toulouse, France; Fax: +33-56133553003 E-mail: karine.philippot@lcc-toulouse.fr

[b] Heteroelements and Transition Metals for Catalysis and Electronic Transfer Group, CNRS; LCC (Laboratoire de Chimie de Coordination); 205 Route de Narbonne, F-31077 Toulouse, France; Fax: +33-56133553003 E-mail: alain.igau@lcc-toulouse.fr

[c] Université de Toulouse; UPS, INPT; LCC; F-31077 Toulouse, France.

[d] CNRS, CEMES (Centre d'Elaboration de Matériaux et d'Etudes Structurales), 29 rue J. Marvig, F-31055 Toulouse, France

† Electronic Supplementary Information (ESI) available: [Size distribution histogram for **Ru1**, TEM images of *N*-phosphanylamidine-stabilized ruthenium nanoparticles **Ru2** and **Ru5** and their corresponding size histograms].
See DOI: 10.1039/b000000x/

1 G. Schmid, *Nanoparticles: From theory to application*, Wiley-VCH, Weinheim, 2004.

2 K. Philippot and B. Chaudret, in *Comprehensive Organometallic Chemistry* III, R. H. Crabtree & M. P. Mingos (Eds-in-Chief), Elsevier, Volume 12 – Applications III: Functional Materials, Environmental and Biological Applications, Dermot O'Hare (Volume Ed.), 2007, Chapter 12-03, 71–99.

3 D. Astruc, *Nanoparticles and Catalysis*, Wiley-VCH, Weinheim, 2008.

4 C. Pan, K. Pelzer, K. Philippot, B. Chaudret, F. Dassenoy, P. Lecante, M.-J. Casanove, *J. Am. Chem. Soc.* 2001, *123*, 7584–7593.

5 J. García-Antón, M. Rosa Axet, S. Jansat, K. Philippot, B. Chaudret, T. Pery, G. Buntkowsky, H.-H. Limbach, *Angew. Chem. Int. Ed.* 2008, *47*, 2074–2078.

6 A. Gual, M.Rosa Axet, K. Philippot, B. Chaudret, A. Denicourt-Nowicki, A. Roucoux, S. Castillón, C. Claver, *Chem. Commun.* 2008, 2759–2761.

7 I. Favier, S. Massou, E. Teuma, K. Philippot, B. Chaudret, M. Gomez, *Chem. Commun.* 2008, 3296–3298.

8 P.-J. Debouttière, V. Martinez, K. Philippot, B. Chaudret, *Dalton Trans.* 2009, 10172–10174.

9 T. D. Le, M.-C. Weyland, Y. El-Harouch, D. Arquier, L. Vendier, K. Miqueu, J.-M. Sotiropoulos, S. Bastin, A. Igau, *Eur. J. Inorg. Chem.* 2008, 2577–2583.

10 T. D. Le, D. Arquier, K. Miqueu, J.-M. Sotiropoulos, Y. Coppel, S. Bastin, A. Igau, *J. Organomet. Chem.* 2009, *694*, 229–236.

11 R. Maura, J. Steele, L. Vendier, D. Arquier, S. Bastin, M. Urrutigoïty, P. Kalck, A. Igau, *J. Organomet. Chem.* 2011, *696*, 897–904.

12 D. Arquier, L. Vendier, K. Miqueu, J.-M. Sotiropoulos, S. Bastin, A. Igau, *Organometallics* 2009, *28*, 4945–4957.

13 Note that the chemical shift of L1 (δ^{31}P 54.3 ppm) and L2 □δ^{31}P 47.1 ppm), typical for P(III)-phosphorus compounds with a P–N linkage, is not affected to any great extend upon coordination to a transition metal

14 a) F. Dornhaus, M. Bolte, H.-W. Lerner, M. Wagner, *Eur. J. Inorg. Chem.* 2006, 1777–1785; b) I. J.Colquhoun, H. C. E. McFarlane, W. McFarlane, *J. Chem. Soc., Chem. Commun.* 1982, 220–221

15 a) Ö. Metin, S. Sahin, S. Özkar, *Int. J. Hydrogen Energy* 2009, *34*, 6304–6313.; b) E. Renbutsu, S. Okabe, Y. Omura, F. Nakatsubo, S. Minami, Y. Shigemasa, H. Saimoto, *Int. J. Biol. Macromol.* 2008, *43*, 62–68 and references therein.

16 For P=O coordination on ruthenium complexes see for exemple : a) V. Cadierno, J. Diez, J. Garcia-Alvarez, J. Gimeno, J. Rubio-Garcia, *Dalton Trans.* 2008, 5737–5748; b) P. W. Cyr, S. J. Rettig, B. O. Patrick, B. R. James, *Organometallics* 2002, *21*, 4672–4679; c) J. W. Faller, B. P. Patel, M. A. Albrizzio, M. Curtis, *Organometallics* 1999, *18*, 3096–3104.

17 P. Pertici, G. Vitulli, *Inorg. Synth.* 1983, *22*, 178–179.